

**GEOELECTRIC INVESTIGATION OF THE GROUNDWATER POTENTIAL IN FEDERAL UNIVERSITY OF TECHNOLOGY AREA, IKOT ABASI, AKWA IBOM STATE, NIGERIA**

Samuel T. Ebong  
Winner M. Umah  
John A. Efiang  
Grace P. Umoren

*Department of Physics, Akwa Ibom State University,  
Ikot Akpaden, Akwa Ibom State*

&

Ekaette S. Attai

*Department of Physics, Collage of Art and Science,  
Ikono L.G.A, Akwa Ibom State, Nigeria.  
Email:siphysicsonline@gmail.com*

<https://doi.org/10.60787/AASD-v1i2-24>

**Abstract**

Geoelectric measurements using the Vertical Electrical Sounding (VES) method were carried out in Federal University of Technology Area, Ikot Abasi, Akwa Ibom State, Nigeria, using the Integrated Geo Instruments and services resistivity meter (IGIS) Terrameter (SAS 1000). The objectives of the study were to investigate the aquifer characteristics and groundwater potential of the subsurface formations. Ten (10) profiles were carried out using the Schlumberger array configuration for the mapping of the prospect, with maximum current electrode separation of 200m. The data was interpreted using the conventional curve matching and computer iteration methods. The data was interpreted using the WinRESIST and computer iteration methods to obtain the resistivity, thickness and depth of the subsurface. Results show that four major curve types were identified, namely: A, H, K and Q depending on the resistivity distribution with depth. The area was observed to have 3 to 4 geoelectric layers. The third layer for VES 1 and VES 2 has a thickness of 71.8m and 66.5m; while, VES 3, VES 5 and VES 7 at the second layer have 56.3m, 66.3m and 51.1m respectively. Generally, the study area has a thickness range of 50m to 80m. The lowest value of the bulk resistivity is  $18.1\Omega m$  and the highest value is  $1412.3\Omega m$ , for VES 10 and VES 4 respectively. VES stations 1,2,3,5,7,8,9 and 10 are the locations that will be recommended for deep well sitting, because they have highest thickness of both weathered zone and fractured zone respectively which are good for groundwater storage.

**Key words:** Groundwater, geoelectric measurement, aquifer, layers and thickness.

## Introduction

Groundwater exploration is gaining more and more importance in Nigeria owing to the ever increasing demand for water supplies, especially in areas with inadequate surface water supplies. Already, ten percent of the world's population is affected by chronic water scarcity and this is likely to rise to one-third by about 2025 (WHO, 1996). The water scarcity experienced by the people, led to the search for surface water supply. Surface water mostly occurs as rivers are subjected to pollution. It is sad to say that most of the rivers in Nigeria are highly polluted, the pollutants being inadvertently introduced by man via industrial and petroleum exploration activities. Despite the reported favourable ground water situations the world over, the Nigeria situation appears to be restricted by the fact that more than half of the country is underlain by sedimentary formations. The main rock types in this geological terrain include igneous and metamorphic rock such as migmatites and granite gneisses. Dan-Hassan and Olorunfemi (1999) used the electrical resistivity method to delineate different subsurface geo-electrical layers, aquifer unit and their characteristics, the subsurface structure and its influence on the general hydro-geological condition in the north central part of Kaduna state, Nigeria.

The Electrical resistivity method is used in the determination of depth to bedrock and nature of superficial deposit and structural mapping. The boundary of the aquifer and zones of high yield potential have been determined (Emmanuel O. Joshua, *et al.*, (2011). The electrical resistivity method is the most widely used geophysical method in the basement terrain. Olayinka (1990) used a multi-electrode resistivity profiling array for groundwater. Ojo et al (1990) in geophysical survey of a dam has employed this method in imaging the distribution of electrical properties of hydro-geological and dam site investigation. This method has also been used to delineate two shallow aquifer units in coastal plain of Okitipupa area, Southwestern Nigeria by Omosuyi *et al.*, (2008). The search for ground water is faced with lots of uncertainties; to minimize or avoid failures altogether, it is pertinent that the right exploration techniques are utilized in the delineation of subsurface water-bearing formations (Coker et al., 2009).

Ikot Abasi, is one the largest city in Akwa Ibom State and in sub-Saharan Africa with the largest urban centre with several settlement (Figure 1), is not just large in area but equally thickly populated which lies within latitudes  $4^{\circ}30'$  and  $5^{\circ}30'$  N and longitudes  $7^{\circ}15'$  and  $8^{\circ}30'$  E (Attai. *et al.*, 2015). This study was carried out at the Federal University of Technology, Ikot Abasi (FUTIA) Figure 2. The study area lies within the southwestern part of the Nigerian Precambrian basement complex and within latitudes  $4^{\circ}30'$  and  $4^{\circ}42'$  N and longitudes  $7^{\circ}30'$  and  $7^{\circ}54'$  E. Three major landform units, namely the hills, plains and river valleys, according to (Ebong and Akpabio (2013); Ebong *et al.*, (2013); Ebong, *et al.*, 2014; Ebong, *et al* (2016)) this dominates the study area. The hills are the most striking feature, although they constitute less than 15% of the total surface area. The plains are the most extensive landform system in the area, with the elevation ranging between 118 and 260 m above sea level with an average elevation of 240 m above sea level which shows a positive correlation with ground water level elevation, that is the hydraulic gradient. Thus, the elevation of the study area is connected to the closeness of the basement complex rocks of the surface (Ebong, *et al.*, 2016). The quaternary sediments in the study area give rise to alluvial plains as well as the beach ridge sands. The alluvial plains include mangrove mudflats, which area under the influence of tidal brackish waters along the coast and in the estuaries of rivers and creeks.. The tertiary coastal plain sand or Calabar Formation is older and consists of beds of unconsolidated coarse textured sandstones, inter-bedded with layers of fined grained massive day (ALSCON, 1997).

In this present study, the aquifer characteristics and groundwater potential of the subsurface formations was studied. Ten (10) profiles were carried out using the Schlumberger array configuration for the mapping of the prospect with maximum current electrode separation of 200m.



Figure 1: Map of Akwa Ibom State indicating the study location, (Attai. et al., 2015)

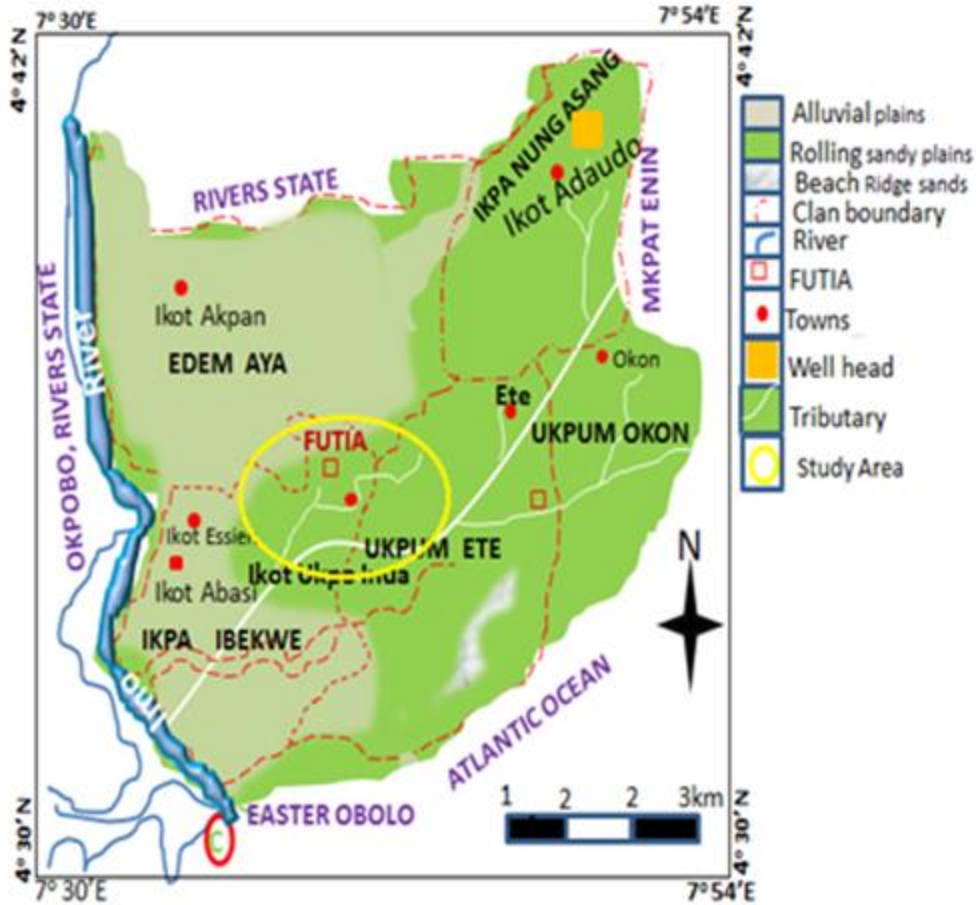


Figure 2: Map of the study location FUTIA

**Theoretical Framework**

The theoretical basis of the dc electrical resistivity method is provided by an elementary consideration of the nature of current and potential distribution in a homogeneous, isotropic medium and a further projection of the analysis to models that fit the actual description of the earth, or very nearly so. For most materials, the physical principle that explains the method of conduction of direct current is embodied in Ohm’s law. This law is expressed mathematically in terms of the electrical resistance R as follows:

$$R = \frac{V}{I} \tag{1}$$

Where I and V are the current and potential difference across the material respectively. To broaden this concept of electrical resistance so that it can be applied to current fields in voluminous media, such as the earth, an alternative expression of Ohm’s law, called the differential form of Ohm’s law is required. This equation gives a relationship between the current density J and the electric field E i.e.

$$\vec{J} = \sigma \vec{E} = \frac{\vec{E}}{\rho} \tag{2}$$

$\sigma$  is the conductivity and its reciprocal,  $\rho$ , is the resistivity, also called specific resistance. Apart from Ohm's law, another consideration needed to arrive at the equation of the potential V about a single point source in a homogeneous earth is the divergence condition:

$$\nabla \cdot \vec{j} = 0 \tag{3}$$

The equation provides a condition that all the current entering one side of a portion of the homogeneous earth must leave the other side, unless there is a current source or sink within the said portion, that is, the divergence of the current density does not occur at any other place except at the current source.

The relationship between the current I and current density J through an area A is

$$I = \vec{j}A \tag{4}$$

$$\text{but } \vec{E} = -\nabla V \tag{5}$$

Hence, from equations (2), (4) and (5),

$$I = -\frac{\nabla V}{\rho}A \tag{6}$$

From equation (1), (2) and (5), one can write that

$$\nabla \cdot \vec{j} = \frac{1}{\rho} \nabla \cdot \vec{E} = -\frac{1}{\rho} \nabla^2 V = 0$$

( $\rho$  being constant). Implying that

$$\nabla^2 V = 0 \tag{7}$$

Equation (7) is Laplace's equation which can be written in spherical polar coordinates as

$$\frac{\partial}{\partial r} \left( r^2 \frac{\partial V}{\partial r} \right) + \frac{1}{r^2 \sin \theta} \frac{\partial}{\partial \theta} \left( \sin \theta \frac{\partial V}{\partial \theta} \right) + \frac{1}{r^2 \sin^2 \theta} \frac{\partial^2 V}{\partial \theta^2} = 0 \tag{8}$$

For a single current source, the potential can be assumed to be with respect to  $\theta$  and  $\phi$  direction so that the derivatives,  $\frac{\partial v}{\partial \theta}$  and  $\frac{\partial^2 v}{\partial \theta^2}$ , are zero and the potential variation will be due only to the distance r from the source as below:

$$\frac{\partial}{\partial r} \left( r^2 \frac{\partial V}{\partial r} \right) = 0 \tag{9}$$

Integration of equation (9) gives

$$v = -\frac{B}{r} + c \tag{10}$$

At a great distance, from the source,  $v = 0$  and the constant, c, will be zero. The constant, B, can be evaluated in terms of the total current flowing across a hemispherical surface of area A ( $A = 2\pi r^2$ ). from equation (6),

$$I = -\frac{2\pi r^2}{\rho} \nabla v$$

$$I = -\frac{2\pi r^2}{\rho} \frac{dv}{dr}$$

$$dv = -\frac{I\rho dr}{2\pi r^2}$$

$$V = \int dv = \int -\frac{I\rho}{2\pi r^2} dr = -\frac{I\rho}{2\pi} \int \frac{dr}{r^2} = -\frac{I\rho}{2\pi r} = V \quad - \quad - \quad - \quad - \quad - \quad - \quad - \quad 11$$

Differentiating (10) gives

$$\frac{dv}{dr} = \frac{B}{r^2}$$

Hence,  $I = -\frac{2\pi r^2}{\rho} \left(\frac{B}{r^2}\right)$

$$= -\frac{2\pi B}{\rho}$$

$$B = -\frac{I\rho}{2\pi} \quad - \quad - \quad - \quad - \quad - \quad - \quad - \quad 12$$

Substituting (11) into (12) (with C=0) gives the potential as

$$V = \frac{\rho I}{2\pi r} \quad - \quad - \quad - \quad - \quad - \quad - \quad - \quad 13$$

Equation 13 is a solution of the Laplace’s equation. Because Laplace’s equation is linear, the sum of two solutions must be a solution. Thus, for two current electrodes where one is a source and the other a sink, the potential at a given point which is a distance  $r_1$  from the source and  $r_2$  from the sink will be the algebraic sum of the potential due to the source and sink respectively, that is

$$V = \frac{I\rho}{2\pi} \left( \frac{1}{r_1} - \frac{1}{r_2} \right) \quad - \quad - \quad - \quad - \quad - \quad - \quad - \quad 14$$

Many geologic situations, such as portrayed by the earth, involves conductivity distribution in a layered medium. The determination of the potential due to a point source in a layered medium involves more rigorous mathematical approaches some of which include the use of geometric optics (based on the assumption that the behaviour of electric currents is similar to light rays) and solving Laplace’s equation with appropriate boundary conditions. The reason for these approaches is that the horizontal layers, which are regarded as having different but homogenous and isotropic electrical properties, introduce some heterogeneity into the ground causing the potential not to have spherical symmetry about the current source as in the case of single homogeneous layer. The potential  $v(r)$  at a distance  $r$  from a point source on the surface of an N-layered earth, based on solving Laplace’s equation with appropriate boundary conditions, can be expressed as

$$V(r) = \frac{I\rho_1}{2\pi} \left( \frac{1}{r} + 2 \int_0^\infty K(\lambda) J_0(\lambda r) d\lambda \right) \quad - \quad - \quad - \quad - \quad - \quad - \quad - \quad 15$$

Where  $k(\lambda)$  is called the kernel function, solely determined by the thicknesses ( $h_1, h_2, \dots, h_N$ ) and resistivities ( $\rho_1, \rho_2, \dots, \rho_N$ ) of the layers, ranging from  $-\infty$  to  $\infty$ ;  $J_0$  (is the Bessel function of the first kind with order zero;  $\lambda$  is a real integration variable ranging from 0 to  $\infty$  with dimension  $l^{-1}$ , and  $\rho_1$  is the resistivity of the top surface layer. A further development of equation (15) using an exponential approximation of kernel functions has been carried out by Niwas and Singhal (1981). Equation (15) and similar

equations have been used in conjunction with equation (13) to calculate the apparent resistivity for any electrode configuration, and to obtain a corresponding album of model curves (called master curves) of apparent resistivity versus electrode spread for a number of layers of different thicknesses. Also, the potential at a distant  $a$  ( $= r$  of equation (15)) from a point source for a simple case of two horizontal layers based on the geometric optics approach is

$$v = \frac{\rho_1 I}{2\pi\beta} \left[ 1 + 2 \sum_{n=1}^{\infty} \frac{K^n}{\left(1 + (2nh/a)^2\right)^{\frac{1}{2}}} \right] \quad - \quad - \quad - \quad - \quad - \quad 16$$

Where  $k = \left(\frac{\rho_2 - \rho_1}{\rho_2 + \rho_1}\right)$  is the refraction coefficient;  $h$  is the thickness of the first layer; and  $\rho_1, \rho_2$ , are resistivities of the first and second layers respectively from equation 16. The apparent resistivity  $\rho_a$  can be written as

$$\rho_a = \rho_1 \left[ 1 + 2 \sum_{n=1}^{\infty} \frac{K^n}{\left(1 + (2nh/a)^2\right)^{\frac{3}{2}}} \right] \quad - \quad - \quad - \quad - \quad - \quad 17$$

This equation has been used to show that for small electrode separation ( $(a \ll h)$ ) the apparent resistivity becomes the resistivity of the upper formation; for large electrode separation ( $a > h$ ) the apparent resistivity is essentially the resistivity of the lower formation; for very conductive lower layer, the resistivity tends to zero; and for resistive substratum, the resistivity of the lower formation increases indefinitely resulting in a line inclined at angle  $45^\circ$  to the horizontal (Okon-Umoren, 1983). The image (geometric optics) method, according to Keller and Frischknecht, (1966), is for too cumbersome to apply to more than one or two layers.

Hence, assuming a solution to Laplace’s equation is regarded a more flexible solution of boundary value problem. In practice, the earth is generally anisotropic. In this situation, the equipotential surfaces are no longer normal to the direction of current flow. Grant and West (1965) have derived the potential for this condition and for the condition of sloping interfaces.

**Materials and Methods**

Ten (10) VES points in three transect were occupied using ABEM Terrameter (SAS1000). Practically, as the distance between the current electrodes is increased about a centre, the total volume of the earth included in the measurement also increases both vertically and laterally. The current electrode half spacing for each survey ranged from a minimum of 5m to a maximum of 200m in progressive steps as a measurement tape was used to measure the electrode spacing. The VES field data obtained were interpreted using the WinResist programme to generate the final model for layer resistivity, thickness and depth to basement.

The apparent resistivity values obtained from field measurements (Tables 1) were plotted against the electrode spacing on bilogarithm coordinates and a preliminary interpretation of each VES curve was carried out using partial curve-matching.

**Table 1:** Summary of VES results and lithology deductions

VES No.	Longitude (Degrees)	Latitude (Degrees)	No. of Layers	Resistivity ( $\Omega$ m)	Thickness (m)	Depth (m)	Lithology
1	7.6067	4.6147	4	1722.9	3.2	3.2	Motley topsoil
				831.7	25.6	28.0	Coarse sand
				202.5	71.8	100.6	Sandy clay
				453.0	-	-	Fine sand
2	7.6087	4.6101	4	457.9	0.6	0.6	Motley topsoil
				1536.3	5.0	5.6	Coarse sand
				553.5	66.5	72.1	Fine sand
				108.8	-	-	Sandy clay
3	7.6096	4.6006	3	1031.5	2.8	2.8	Motley topsoil
				374.6	56.3	59.1	Fine sand
				198.2	-	-	Sandy clay
4	7.6036	4.6067	3	806.8	0.3	0.3	Motley topsoil
				1412.3	28.1	28.4	Coarse sand
				103.9	-	-	Sandy clay
5	7.6052	4.6031	3	1959.2	1.1	1.1	Motley topsoil
				794.4	66.3	67.4	Coarse sand
				206.9	-	-	Sandy clay
6	7.6005	4.5864	3	449.9	6.5	6.5	Motley topsoil
				1151.6	32.6	39.0	Coarse sand
				36.2	-	-	Clay
7	7.6056	4.6012	3	1288.1	2.8	2.8	Motley topsoil
				641.9	51.1	59.2	Fine sand
				55.9	-	-	Clay
8	7.6114	4.5927	3	587.8	2.0	2.0	Motley topsoil
				28.7	37.2	39.2	Clay
				472.2	-	-	Fine sand
9	7.6125	4.5923	3	264.8	2.0	2.0	Motley topsoil
				67.6	30.5	32.5	Clay
				244.1	-	-	Sandy clay
10	4.5896	4.5896	3	370.7	5.0	5.0	Motley topsoil
				18.1	17.9	22.8	Clay
				96.7	-	-	Sandy clay



**Results and Discussion**

Five major curve types were identified, namely: QH, KQ, Q, H, and K as shown in Table 2. VES 3, 5, and 7 are Type Q while VES 8, 7 and 9 are Type H, VES 4 and 6 are Type K, and only VES 1 and 2 are of Type QH and KQ respectively. The apparent resistivity curves reveal a dominant curve Type Q and H over the entire area. The dominant of this curve type shows that a homogenous subsurface succession and in most sounding curves the same layer were found. Figures 3 (a - j), show typical geo-electric curves representative of the curve Types QH, KQ, Q, H and K respectively.

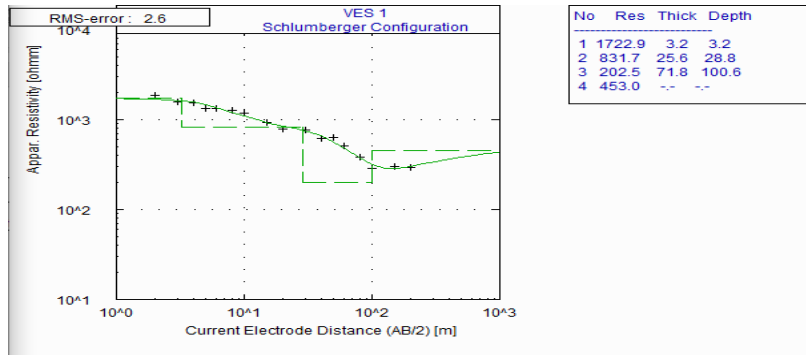


Figure 3a: Interpreted curve for VES 1(Typical QH VES curve type)

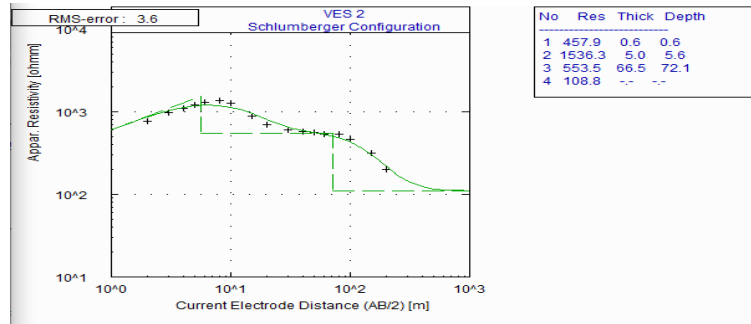


Figure 3b: Interpreted curve for VES 2(Typical KQ VES curve type)

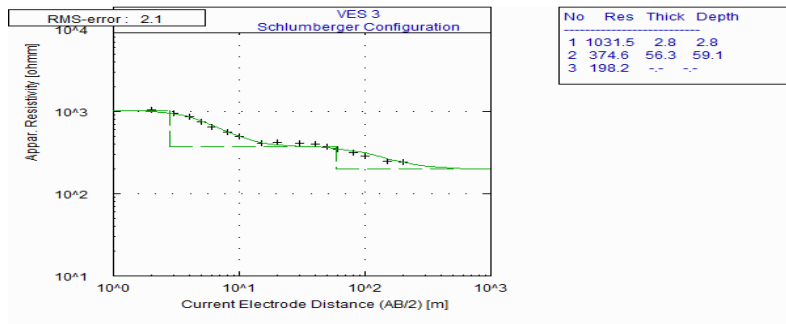


Figure 3c: Interpreted curve for VES 3(Typical Q VES curve type).

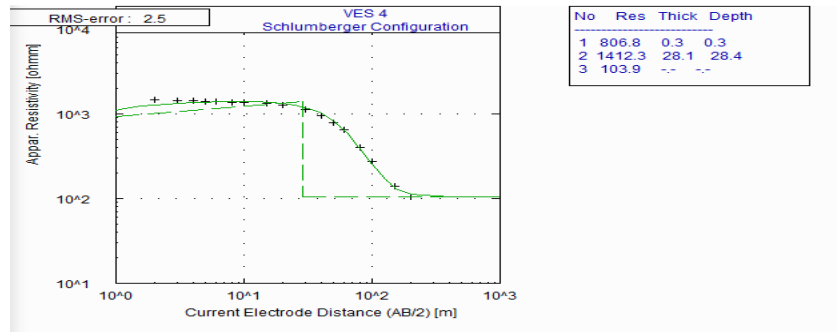


Figure 3d: Interpreted curve for VES 4(Typical K VES curve type)

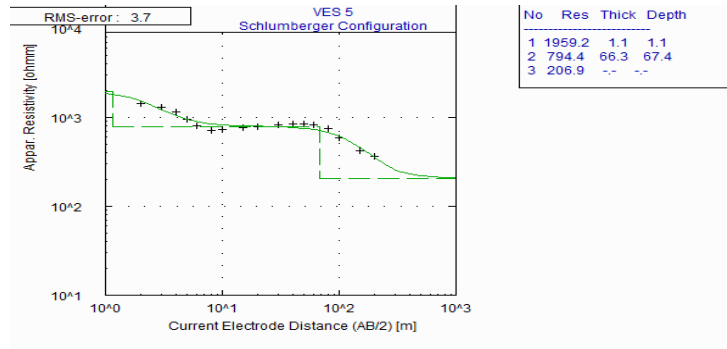


Figure 3e: Interpreted curve for VES 5(Typical Q VES curve type)

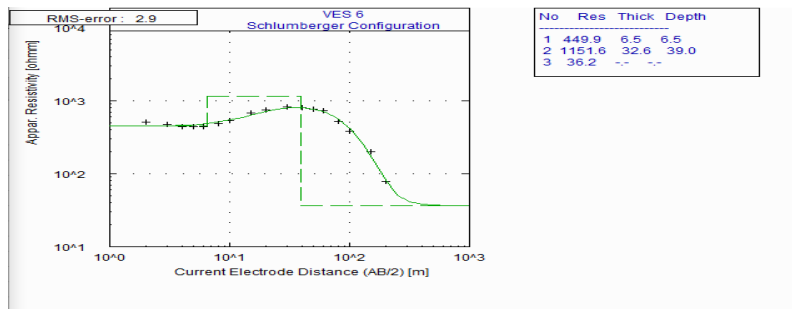


Figure 3f: Interpreted curve for VES 6(Typical K VES curve type)

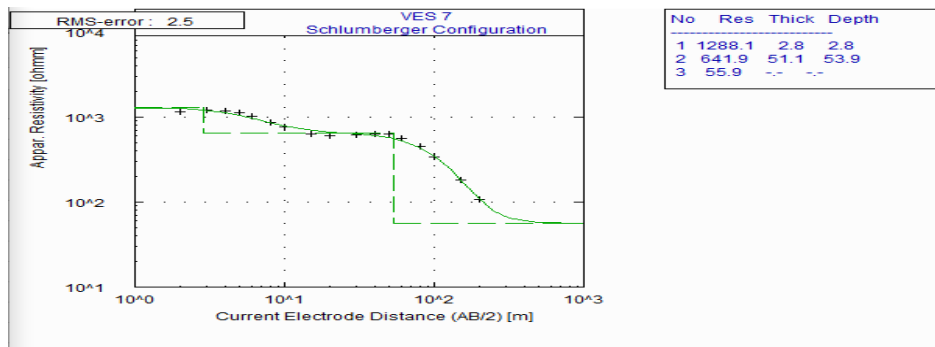


Figure 3g: Interpreted curve for VES 7(Typical Q VES curve type)

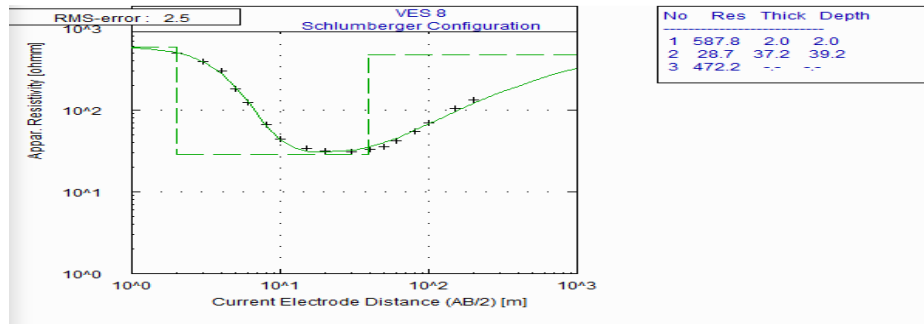


Figure 3h: Interpreted curve for VES 8(Typical H VES curve type)

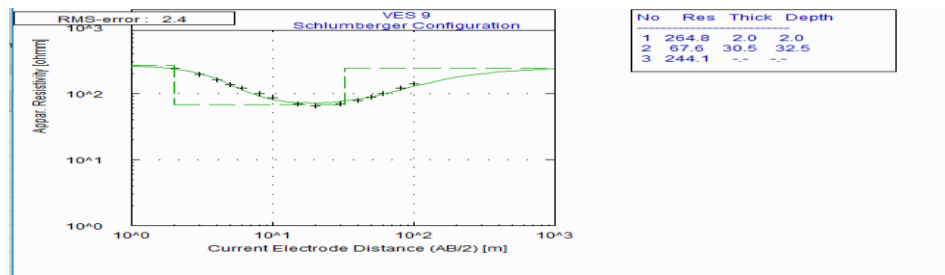


Figure 3i: Interpreted curve for VES 9(Typical H VES curve type)

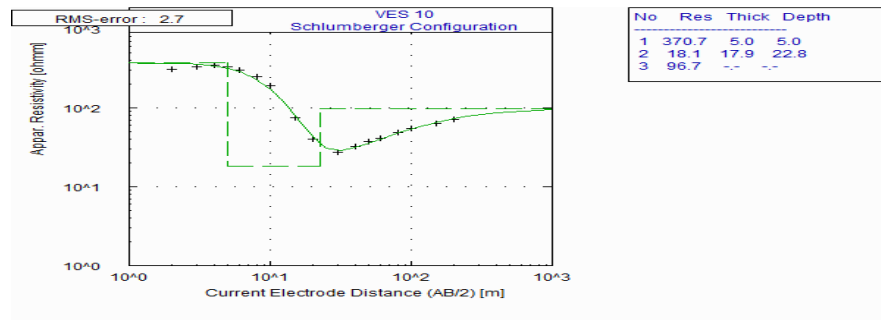


Figure 3j: Interpreted curve for VES 10(Typical H VES curve type)

The sounding curve from the WinRESIST software depicted four geoelectric layers, as seen in Figure 3a. The curve type was identified as QH-type ( $\rho_1 > \rho_2 > \rho_3 < \rho_4$ ). The first layer, which was identified to be a motley top soil, has a resistivity value of 1722.9 $\Omega$ m and a thickness of 3.2m. The second layer consisting of coarse sand has a resistivity of 831.7 $\Omega$ m and a thickness of 23.6m. The third layer, which consisting of fine sand, has a resistivity value 202.5 $\Omega$ m and a thickness of 71.8m. The fourth layer has a resistivity value of 453.0 $\Omega$ m and no defined thickness, because the current sent in was not able to penetrate further due to the electrode spacing. The curve type in Figure 3b was identified as KQ-type ( $\rho_1 < \rho_2 > \rho_3 > \rho_4$ ). The motley topsoil which is the first layer has a resistivity value of 457.9 $\Omega$ m and a thickness of 0.6m. The second layer, consisting of coarse sand, has a resistivity of 1536.3 $\Omega$ m and a thickness of 5.0m. The third layer, which consists of fine sand, has a resistivity value 553.5 $\Omega$ m and a thickness of 66.5m. The fourth layer, identified as sandy clay, has a resistivity value of 108.8 $\Omega$ m and no defined thickness, because the current sent in was not able to penetrate further due to the electrode spacing. The curve type in Figure 3c was identified as Q-type ( $\rho_1 > \rho_2 > \rho_3$ ). The motley topsoil, which is the

first layer, has a resistivity value of 1031.5Ωm and a thickness of 2.8m. The second layer, consisting of fine sand, has a resistivity of 374.6Ωm and a thickness of 56.3m. The third layer, identified as sandy clay, has a resistivity value 198.2Ωm and an undefined thickness. The curve type in Figure 3d was identified as k-type ( $\rho_1 > \rho_2 > \rho_3$ ). The motley topsoil, which is the first layer, has a resistivity value of 806.8Ωm and a thickness of 0.3m. The second layer, identified as coarse sand, has a resistivity of 1412.3Ωm and a thickness of 28.1m. The third layer, which consists of sandy clay, has a resistivity value 103.9Ωm and an undefined thickness. And for the rest of Figures 3e – j as indicating in Table 2.

**Table 2:** Interpreted VES showing different curves type

VES NO.	COORDINATES		RESISTIVITY (Ωm)				THICKNESS (m)			DEPTH (m)			ELEV . (m)	CURVE TYPE	CURVE CHARACTERISTICS
	LONG. (deg.)	LAT. (deg.)	$\rho_1$	$\rho_2$	$\rho_3$	$\rho_4$	$h_1$	$h_2$	$h_3$	$d_1$	$d_2$	$d_3$			
1	7.6067	4.6147	1722.9	831.7	202.5	453.0	3.2	25.6	71.8	3.2	28.0	100.6	15	QH	$\rho_1 > \rho_2 > \rho_3 < \rho_4$
2	7.6087	4.6101	457.9	1536.3	553.5	108.8	0.6	5.0	66.5	0.6	5.6	72.1	9	KQ	$\rho_1 < \rho_2 > \rho_3 > \rho_4$
3	7.6096	4.6006	1031.5	374.6	198.2	-	2.8	56.3	-	2.8	59.1	-	9	Q	$\rho_1 > \rho_2 > \rho_3$
4	7.6036	4.6067	806.8	1412.3	103.9	-	0.3	28.1	-	0.3	28.4	-	7	K	$\rho_1 < \rho_2 > \rho_3$
5	7.6052	4.6031	1959.2	794.4	206.9	-	1.1	66.3	-	1.1	67.4	-	9	Q	$\rho_1 > \rho_2 > \rho_3$
6	7.6005	4.5864	449.9	1151.6	36.2	-	6.5	32.6	-	6.5	39.0	-	9	K	$\rho_1 < \rho_2 > \rho_3$
7	7.6056	4.6012	1288.1	641.9	55.9	-	2.8	51.1	-	2.8	53.9	-	7	Q	$\rho_1 > \rho_2 > \rho_3$
8	7.6114	4.5927	587.8	28.7	472.2	-	2.0	37.2	-	2.0	39.2	-	9	H	$\rho_1 > \rho_2 < \rho_3$
9	7.6125	4.5923	264.8	67.6	244.1	-	2.0	30.5	-	2.0	32.5	-	3	H	$\rho_1 > \rho_2 < \rho_3$
10	4.5896	4.5896	370.7	18.1	96.7	-	5.0	17.9	-	5.0	22.8	-	14	H	$\rho_1 > \rho_2 < \rho_3$

The weathered zone beneath VES 5 has the highest thickness of about 66.3 m and VES 1 having the lowest thickness with about 5.0 m. Thus the thickness of the weathered layer for the study area is high enough to form groundwater accumulation and therefore recommended for a borehole sitting. VES stations 1, 2, 3, 5, 7, 8, 9 and 10 are the locations that will be recommended for groundwater exploitation, because they have highest thickness of both weathered zone and fractured zone respectively which are good for groundwater storage. The groundwater flow regime in the study area suggests the nature and pattern of distribution of the water table in the study area. The major aquifer geo-materials are gravelly sand, fine sand, fine to coarse grained sand and medium-grained sand (Attai. *et al.*, 2015).

**Conclusion**

The results of geo-electric investigation carried out over part of Federal University of Technology (FUTIA), Ikot Abasi Local Government Area revealed maximum of four sub-surface layers: thin top layer, the alluvium, the aquifer and the bedrock respectively.

## References

- Aluminum Smelter Company of Nigeria (ALSCON). (1997): Ikot Abasi - The Aluminum Town: Socio-Economic Transformation of a Nigeria Community.
- Attai, E., Ebong, S., Thaddeus, S., and Joshua, E. (2015): Application of Vertical Electrical Sounding to Investigate the Groundwater Potential in Abak Local Government Area, Akwa Ibom State, Nigeria. *Journal of Geography, Environment and Earth Science International* 3(1): 1-12, Article no.JGEESI.17832 SCIENCEDOMAIN international, [www.sciencedomain.org](http://www.sciencedomain.org)
- Coker JO, Makinde V, Olowofela JA (2009). Geophysical Investigation of Groundwater Potentials of Oke-Badan Estate, Ibadan, Southwestern, Nigeria. Proceedings of 3rd International Conference on Science and National Development University of Agric. Abeokuta, p. 119.
- Dan-Hassan MA, Olorunfemi MO (1999). Hydro-geophysical investigation of a basement terrain in the north central part of the Kaduna state, Nigeria. *J. Min. Geol.*, 35(2): 189-206.
- Ebong, S., and Akpabio, G. (2013): Comparative Study of Electricity and Thermal Conductivity of Three Land Form in Akwa Ibom State. *International Journal of Advance Research, Ijoar. Org.* Volume 1, Issue 8, Online: ISSN 2320-9186 Pp. 1- 14.
- Ebong, S., Ekanem, M., and George, N. (2023): Reservoir Characterisation Using Seismic Inversion Techniques for Mapping of Prospects. *Researchers Journal of Science and Technology (REJOST)* (2023), 3(1): 1 - 13 <https://rejost.com.ng>
- Ebong, S., Attai, E., and Joshua, E. (2016): Measurement of Thermal Conductivity and Specific Heat Capacity of Three Major Geo-morphological Units in Akwa Ibom State, Nigeria. *British Journal of Applied Science & Technology*, 12(2): 1-7, 2016, Article no.BJAST.17834 ISSN: 2231-0843, NLM ID: 101664541 SCIENCEDOMAIN international, [www.sciencedomain.org](http://www.sciencedomain.org)
- Ebong, S., Akpabio, G., and Atai, E. (2013): Comparative Study of Thermal Conductivity and Density of Three Land Forms in Akwa Ibom State. *International Journal of Physics and Applications*, © International Research Publication House. <http://www.irphouse.com>ISSN 0974-3103 Volume 5, Number 2, pp. 83-89.
- Ebong, S., Akpabio, G., Atai, E., Oji, H., and Umoren, E. (2014): Thermal Properties of Three Major Landforms in Akwa Ibom State, Nigeria. *International Research Journal of Pure Applied Physics*, Vol. 2, No.2, Pp. 10-19, June 2014 Published by European Centre for Research Training and Development UK ([www.ea-journals.org](http://www.ea-journals.org)).

- Joshua, E., Odeyemi, O., and Fawehinmi, O. (2011): Geo-electric investigation of the groundwater potential of Moniya Area, Ibadan. *Journal of Geology and Mining Research* Vol. 3(3), pp. 54-62, March 2011. Available online <http://www.academicjournals.org/jgmr>
- Ojo JS, Ayangbesan TA, Olorunfemi MO (1990). Geo-physical Survey of Dam Site: A Case Study. *J. Min. Geol.*, 26(2): 201-206.
- Olayinka AI (1990). Case histories of multi-electrode resistivity profiling array for groundwater in basement complex areas of Kwara state, Nigeria. *J. Min. Geol.*, 26(1): 27-34.
- Omosuyi GO, Ojo JS, Olorunfemi MO (2008). Geo-electric Sounding to Delineate Shallow Aquifer in the Coastal Plain Sands of Okitipupa Area, Southwestern Nigeria. *Pacific J. Sci. Technol.*, 9(2): 562-577.
- World Health Organization(WHO) (1996). *Guidelines for Drinking Water, Vol. 1, Recommendation.* Geneva Switzer